Carbohydrate Polymers 88 (2012) 1470–1475

Contents lists available at SciVerse ScienceDirect

Carbohydrate Polymers

journal homepage: www.elsevier.com/locate/carbpol

Hydrothermal synthesis and characterization of wood powder/$CaCO_3$ composites

Ming-Guo Ma[a,*], Lian-Hua Fu[a], Shu-Ming Li[a], Xue-Ming Zhang[a], Run-Cang Sun[a,b], Yong-Dong Dai[c]

[a] Institute of Biomass Chemistry and Technology, College of Materials Science and Technology, Beijing Forestry University, Beijing 100083, PR China
[b] State Key Laboratory of Pulp and Paper Engineering, South China University of Technology, Guangzhou 510640, PR China
[c] Department of Chemistry, JiuJiang Vocational University, Jiujiang 332200, PR China

ARTICLE INFO

Article history:
Received 10 January 2012
Received in revised form 9 February 2012
Accepted 19 February 2012
Available online 25 February 2012

Keywords:
Wood powder
$CaCO_3$
Composites
Hydrothermal

ABSTRACT

The purpose of this study is to investigate the fabrication of wood powder/$CaCO_3$ composites. In this study, we report a hydrothermal route for the preparation of wood powder/$CaCO_3$ composites using the dewaxed wood powder. The wood powder was pretreated by the NaOH/urea solution. The urea acts as the CO_3^{2-} source and provides a basic condition for the synthesis of $CaCO_3$. The influences of several reaction parameters such as the heating time and the types of additives on the products were investigated by X-ray powder diffraction, Fourier transform infrared spectrometry, scanning electron microscopy, thermogravimetric analysis, and differential thermal analysis. The experimental results demonstrated that the additives not only had an effect on the phases of composites, but also on the microstructure and shape of composites. Moreover, the thermal stability of the samples was also investigated. Compared with cellulose-based composites, the wood powder composites can utilize all the main components of lignocelluloses.

1. Introduction

Wood is a typical biomass material. Wood-based composites are a very promising and sustainable green material to achieve durability without using toxic chemicals. The wood–polymer composites have been extensively explored (Ashori, 2008). Until now, rapid progress has been made in the preparation of wood–polymer composites including wood fiber/polyolefin composites (Selke & Wichman, 2004), wood/polypropylene composites (Stark & Rowlands, 2003), wood/polyethylene flour composites (Lai, Yeh, Wang, Chan, & Shen, 2003), wood/poly(vinyl chloride) composites (Jiang & Kamdem, 2004), wood/plastic composites (Okamoto, 2003). However, there have been only few literatures reporting on the synthesis of wood powder/inorganic composites. The introduction of inorganic materials into wood matrix maybe significantly improves the performance of composites (Blanchard & Blanchet, 2011; Mai & Militz, 2004). SiO_2 wood/inorganic composites with good antimicrobial properties have been prepared by the sol–gel process with water-soluble silicon oligomer agents (Fujita, Miyafuji, & Saka, 2003). Miyafuji, Kokaji, and Saka (2004) reported the preparation of wood/inorganic composites with improved photostability by the sol–gel process with UV absorbent. Bakraji and Salman (2003) found that the inorganic additives had a positive effect on the compression strength of wood/plastic composites from Syrian tree species using gamma-ray irradiation.

$CaCO_3$ is an important inorganic material. The researches of the cellulose/$CaCO_3$ (calcite) composites have been reported (Dalas, Klepetsanis, & Koutsoukos, 2000; Fimbel & Siffert, 1986; Shen, Song, Qian, & Yang, 2010; Subramanian, Maloney, & Paulapuro, 2005). More recently, Vilela et al. (2010) prepared cellulose/$CaCO_3$ bionanocomposite by the controlled reaction of $CaCl_2$ with dimethylcarbonate ($(CH_3)_2CO_3$) in alkaline medium in the presence of cellulose fibers. To date, however, there has been no report on the research of wood powder/$CaCO_3$ composites prepared by hydrothermal method, which provides unique temperature–pressure environments and has advantage of controlling morphology of the products by adjusting the reaction parameters (Cundy & Cox, 2003). In previous studies, we synthesized cellulose/carbonated hydroxyapatite composites (Jia, Li, Ma, Sun, & Zhu, 2010) and cellulose/$CaCO_3$ composites (Jia, Li, Ma, Sun, & Zhu, 2012) with good biocompatibility in NaOH/urea solution by hydrothermal method. The experimental results indicated that the hydrothermal method favored the fabrication of biomass materials. As we know, the main components of lignocelluloses are cellulose, hemicelluloses, and lignin. Cellulose is obtained by the extraction and isolation of lignocellulosic biomass, which needs long reaction time and complex steps. The wood powder/$CaCO_3$ composites can utilize all the main components of lignocelluloses, compared with the cellulose/$CaCO_3$ composites.

Herein, we report the synthesis of the wood powder/$CaCO_3$ composites by hydrothermal method using the dewaxed wood powder. The urea acts as the CO_3^{2-} source and provides a basic condition for the synthesis of $CaCO_3$. The influences of several reaction parameters such as the heating

* Corresponding author. Tel.: +86 10 62336592; fax: +86 10 62336972.
E-mail address: mg_ma@bjfu.edu.cn (M.-G. Ma).

0144-8617/$ – see front matter © 2012 Elsevier Ltd. All rights reserved.
doi:10.1016/j.carbpol.2012.02.043

time and the types of additives on the products were also investigated.

2. Experimental

2.1. Preparation of wood powder/$CaCO_3$ composites

All chemicals were of analytical grade and used as received without further purification. All experiments were conducted under air atmosphere. In a typical experimental, 7.00 g of NaOH and 12.00 g of urea were added into 81 mL of distilled water under vigorous stirring to form NaOH–urea aqueous solution. Then, 1 g of dewaxed wood powder was added into the above solution under vigorous stirring. The above solution was cooled to −12 °C for 12 h. The obtained solution was used for the preparation of wood powder/$CaCO_3$ composites.

For the synthesis of wood powder/$CaCO_3$ composites, 10 mL of $C_4H_6O_4Ca{\cdot}H_2O$ solution (0.10 mol/L) and 10 mL of Na_2CO_3 solution (0.10 mol/L) were added into the above obtained solution (20 mL) under vigorous stir. The mixture solution was transferred into a 50-mL Teflon-lined stainless steel autoclave. The autoclave was maintained at 160 °C for a certain time (2 h, or 12 h, or 24 h). The product was separated from the solution by centrifugation, washed by water and ethanol three times, and dried at 60 °C for further characterization.

For comparison, the samples were also fabricated by hydrothermal method at 160 °C for a certain time (2 h, or 12 h, or 24 h) using NaH_2PO_4 solution (10 mL, 0.06 mol/L) and $(NH_4)_2SO_4$ solution (10 mL, 0.10 mol/L) instead of Na_2CO_3 solution (10 mL, 0.10 mol/L), respectively, and kept the other conditions the same.

2.2. Characterization

X-ray powder diffraction (XRD) was performed in 2θ range from 10° to 70° on a Rigaku D/Max 2200-PC diffractometer with Cu Kα radiation (λ = 0.15418 nm) and graphite monochromator at ambient temperature. Fourier transform infrared (FTIR) spectroscopy was carried out on an FTIR spectrophotometer (Nicolet 510) in a range of wavenumber from 4000 to 400 cm^{-1}, using the KBr disk method. Scanning electron microscopy (SEM) images were recorded with a Hitachi 3400N scanning electron microscopy. All samples were Au coated prior to examination by SEM. Thermal behavior of the samples was tested using thermogravimetric analysis (TGA) and differential thermal analysis (DTA) on a simultaneous thermal analyzer (DTG-60, Shimadzu) from room temperature to 600 °C at a heating rate of 10 °C min^{-1} in flowing air.

3. Results and discussion

3.1. The phases, microstructure, and shapes of wood powder/$CaCO_3$ composites

The dewaxed wood powder consisted of cellulose, hemicellulose, and lignin. However, only the cellulose was crystallinity. Therefore, one can see the diffraction peak of cellulose at $2\theta = 21.7°$ in Fig. 1. All the other diffraction peaks are indexed to well-crystallized calcite with a hexagonal structure (JCPDS 47-1743). No peaks from impurities such as aragonite were observed. When the heating time was only 2 h, the peaks intensity was strong. The Ca^{2+} and CO_3^{2-} reacted rapidly at high temperature, inducing the nucleation and growth of $CaCO_3$. These results confirmed that the hydrothermal method had advantage of preparing highly crystalline products.

FTIR has been proved to be useful for studying functional groups of samples, as shown in Fig. 2. One can see that a peak at 1038 cm^{-1}

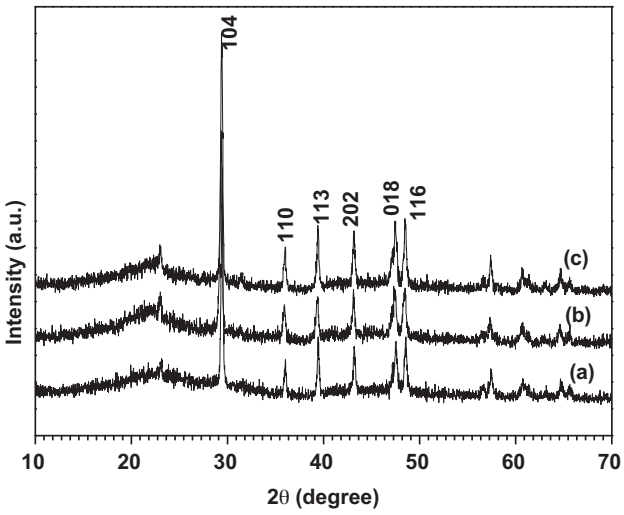

Fig. 1. XRD patterns of the wood powder/$CaCO_3$ composites prepared by hydrothermal method at 160 °C for different times: (a) 2 h; (b) 12 h; (c) 24 h.

can be attributed to C—O—C pyranose ring skeletal vibration of cellulose. The strong peak at 1434 cm^{-1} is characteristic of ν_{3-3} CO_3^{2-} and ν_{3-4} CO_3^{2-} (He, Huang, Liu, Chen, & Xu, 2007; Nelson & Featherstone, 1982), further indicating the existence of $CaCO_3$ in composites. Furthermore, one can clearly see the characteristics of calcite at 702 cm^{-1} and 878 cm^{-1} (Donners et al., 2000). The peak intensity of characteristics become stronger due to the highly crystalline, compared with the previous study (Jia et al., 2012). These results were consistent with the XRD results, further indicating that the polymorph of obtained $CaCO_3$ in composites was calcite.

The morphologies and microstructures of the wood powder/$CaCO_3$ composites were investigated by SEM. The SEM images of the samples synthesized by hydrothermal method were shown in Fig. 3. One can see that the $CaCO_3$ grows on the surface of wood powder. Magnified micrographs of the composites were shown in Fig. 3b, d, and f. When the heating time was 2 h, $CaCO_3$ particles were dispersed on the surface of wood powder (Fig. 3a and b). When the heating time was increased from 2 h to 12 h, $CaCO_3$ with six-side-like shape were dispersed on the surface of wood powder (Fig. 3c and d). Interestingly, pores were observed around the center of $CaCO_3$ congregates. When the heating time

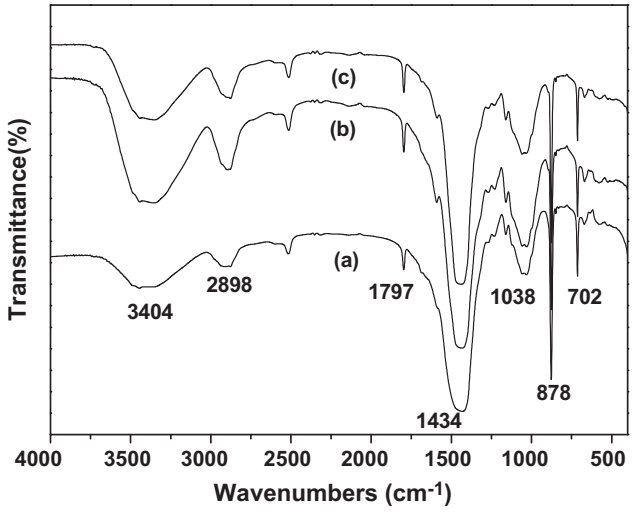

Fig. 2. FTIR spectra of the wood powder/$CaCO_3$ composites prepared by hydrothermal method at 160 °C for different times: (a) 2 h; (b) 12 h; (c) 24 h.

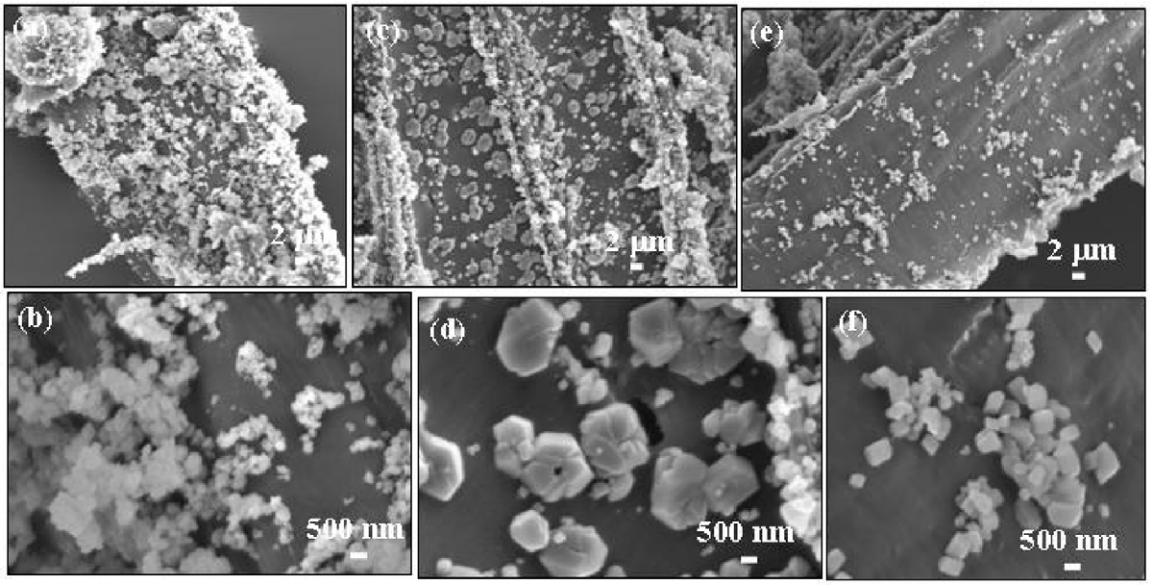

Fig. 3. SEM images of the wood powder/$CaCO_3$ composites prepared by hydrothermal method at 160 °C for different times: (a and b) 2 h; (c and d) 12 h; (e and f) 24 h.

was increased to 24 h, $CaCO_3$ with cube-like morphology were dispersed on the surface of wood powder (Fig. 3e and f). As we all know, the cube is typical shape of calcite. Moreover, the size of $CaCO_3$ increased and the number of $CaCO_3$ decreased with increasing heating time. Of all the growth mechanisms, one basic crystal growth mechanism in solution systems is the well-known "Ostwald ripening process" (Sugimoto, 1987), in which the larger particles will grow at the expense of the smaller ones. In view of the experimental results, we propose that the growth may follow the "Ostwald ripening process".

3.2. The influences of additives on the phases and shapes of wood powder/$CaCO_3$ composites

We also investigated the effects of additives on the phases and morphologies of the samples. The original purpose is to synthesize the wood powder/hydroxyapatite composites and the wood powder/$CaSO_4$ composites using NaH_2PO_4 and $(NH_4)_2SO_4$ instead of Na_2CO_3, respectively. However, when the NaH_2PO_4 was used to instead of Na_2CO_3, the XRD patterns of the samples were indexed of the wood powder/$CaCO_3$ (majority phase) composites (Fig. 4A). Only when the heating time was increased to 24 h, a small diffraction peak of hydroxyapatite at $2\theta = 32.1°$ was observed as a minor phase (Fig. 4A(c)). Moreover, the peaks intensity of calcite increased with increasing heating time. The solubility product (*Ksp*) of $CaCO_3$ is 2.8×10^{-9}, which is bigger than that of $Ca_3(PO_4)_2$ (2.0×10^{-29}). As we all know, the product is first obtained with low *Ksp* value under normal condition. Therefore, the obtained products should not be the wood powder/$CaCO_3$ composites, but wood powder/$Ca_3(PO_4)_2$ or hydroxyapatite composites. However, the final products were the wood powder/$CaCO_3$ composites. These results were due to the existence of urea with high concentration, which decomposed at high temperature and acted as the CO_3^{2-} source for the synthesis of $CaCO_3$. CO_3^{2-} with high concentration favored the preparation of $CaCO_3$ and restrained the fabrication of hydroxyapatite. When the long heating time was applied, hydroxyapatite was observed (Fig. 4A(c)).

Using $(NH_4)_2SO_4$ instead of Na_2CO_3, the wood powder/$CaCO_3$ composites were observed, as shown in Fig. 4B. Firstly, urea with high concentration acted as the CO_3^{2-} source for the synthesis of $CaCO_3$. Moreover, the solubility product (*Ksp*) of $CaCO_3$ is 2.8×10^{-9}, which is smaller than that of $CaSiO_3$ (9.1×10^{-6}). The

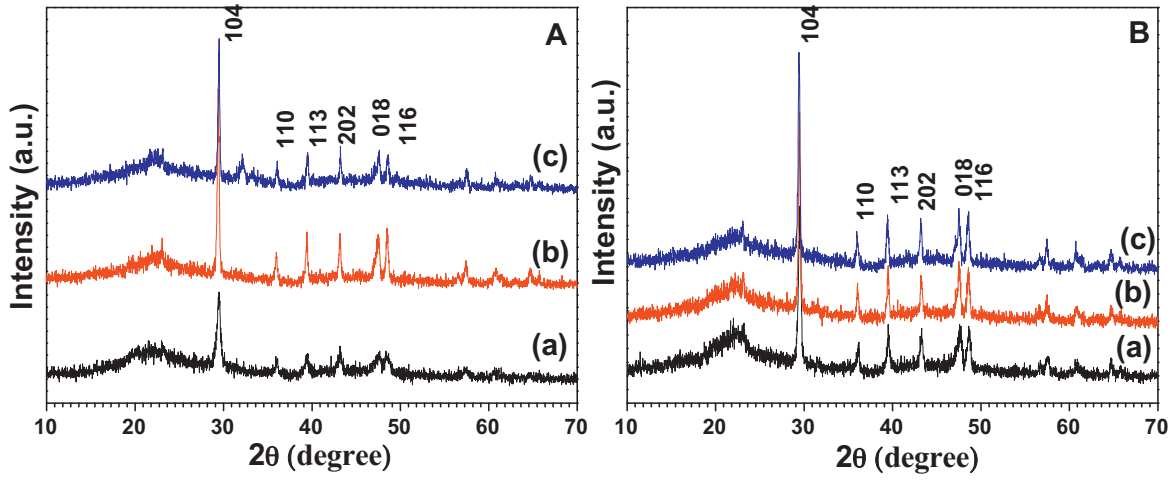

Fig. 4. XRD patterns of the wood powder/$CaCO_3$ composites prepared by hydrothermal method using (A) NaH_2PO_4 and (B) $(NH_4)_2SO_4$ at 160 °C for different times: (a) 2 h; (b) 12 h; (c) 24 h.

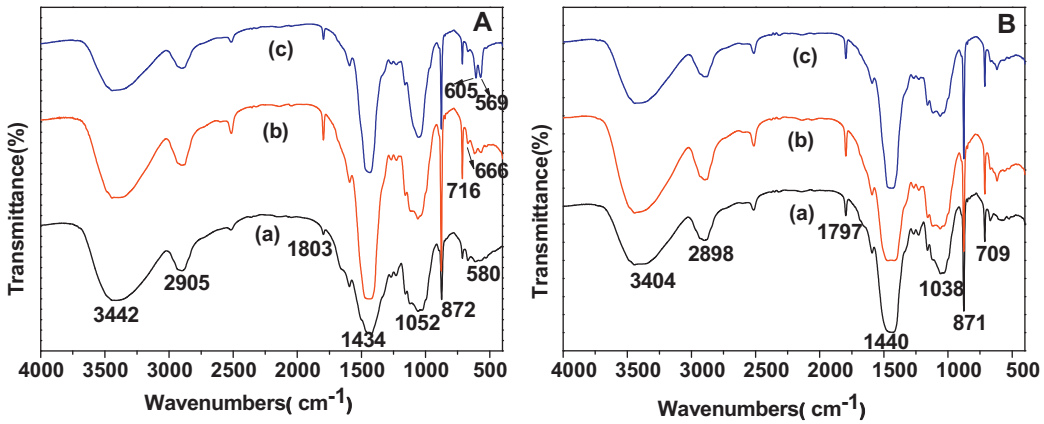

Fig. 5. FTIR spectra of the wood powder/$CaCO_3$ composites prepared by hydrothermal method using (A) NaH_2PO_4 and (B) $(NH_4)_2SO_4$ at 160 °C for different times: (a) 2 h; (b) 12 h; (c) 24 h.

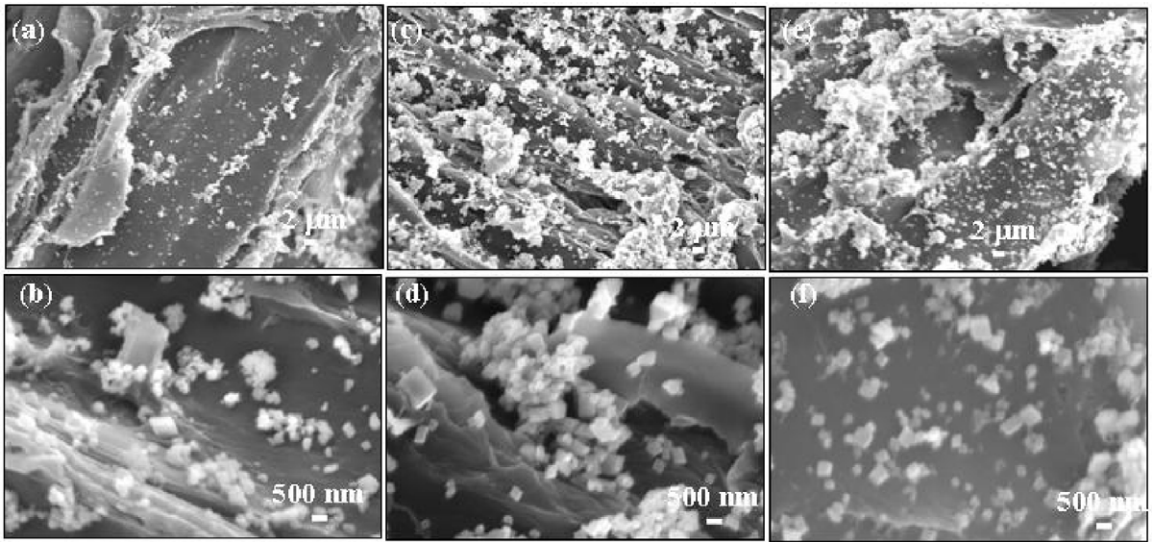

Fig. 6. SEM images of the wood powder/$CaCO_3$ composites prepared by addition of NaH_2PO_4 at 160 °C for different times: (a and b) 2 h; (c and d) 12 h; (e and f) 24 h.

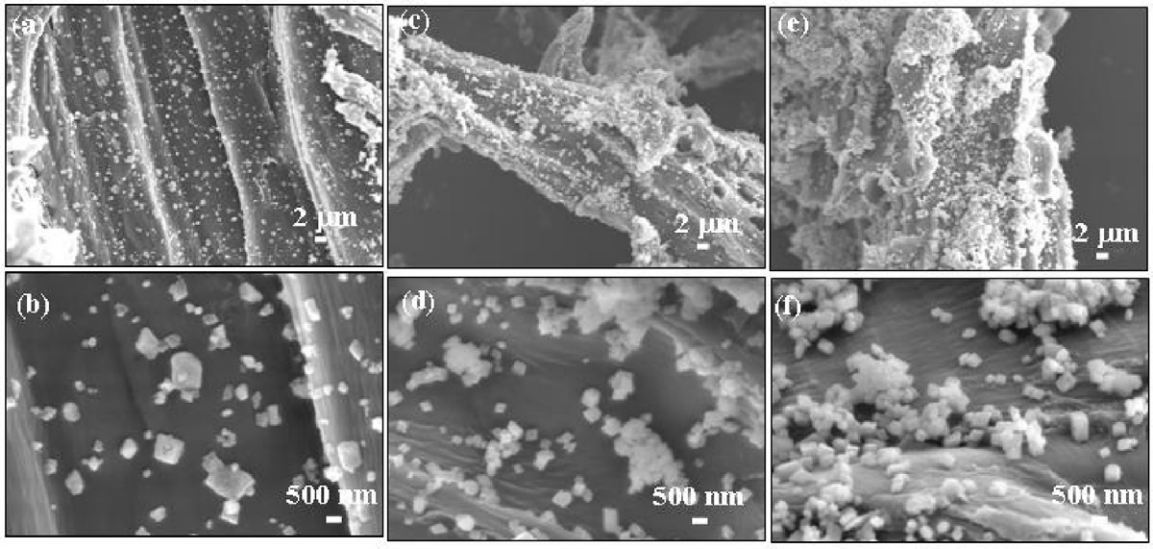

Fig. 7. SEM images of the wood powder/$CaCO_3$ composites prepared by the addition of $(NH_4)_2SO_4$ at 160 °C for different times: (a and b) 2 h; (c and d) 12 h; (e and f) 24 h.

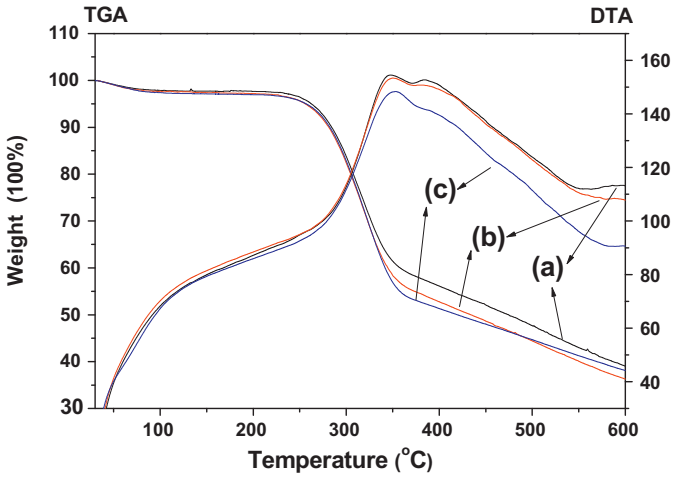

Fig. 8. TGA and DTA curves of the wood powder/$CaCO_3$ composites prepared by the addition of (a) NaH_2PO_4, (b) Na_2CO_3, and (c) $(NH_4)_2SO_4$.

product is first obtained with low *Ksp* value under normal condition. Therefore, the obtained products are not the cellulose/$CaSO_4$ composites, but cellulose/$CaCO_3$ composites. Furthermore, the peak intensity became stronger, compared with Fig. 4A. The $CaCO_3$ was fabricated in a basic condition and the existence of $(NH_4)_2SO_4$ favored the increasing of pH by providing the NH_4^+. Therefore, the growth mechanism of $CaCO_3$ was difference between the additives of $(NH_4)_2SO_4$ and NaH_2PO_4.

All of the samples synthesized by the additives of NaH_2PO_4 and $(NH_4)_2SO_4$ have similar FTIR spectra, compared with Fig. 2, as shown in Fig. 5. All of the characteristics of $CaCO_3$ and cellulose were observed. The peak at 1052 or 1038 cm^{-1} can be attributed to C—O—C pyranose ring skeletal vibration of cellulose. The strong peak at 1434 or 1440 cm^{-1} is characteristic of ν_{3-3} CO_3^{2-} and ν_{3-4} CO_3^{2-} (He et al., 2007; Nelson & Featherstone, 1982). The strong bands at 872 and 716 cm^{-1}, or 871 and 709 cm^{-1} are indicative of the characteristics of calcite (Donners et al., 2000), further indicating that the phase of the $CaCO_3$ is calcite. Moreover, from the FTIR spectra in Fig. 5A, the band at 666 cm^{-1} belongs to the liberation mode of the OH— vibration in hydroxyapatite (Jokanović et al., 2006) and the intense peaks located at 605 and 569 cm^{-1} are assigned to PO_4^{3-} (Kuriakosea et al., 2004), implying the existence of hydroxyapatite. These results were consistent with the XRD results in Fig. 4.

The corresponding SEM images of samples using the additives of NaH_2PO_4 and $(NH_4)_2SO_4$ were shown in Figs. 6 and 7, respectively. From which one can see that the $CaCO_3$ had cube-like shape and dispersed on the surface of wood powder. The number of $CaCO_3$ cubes and congregates increased with increasing heating time. This result was different from the previous result in Fig. 3, in which the number of $CaCO_3$ decreased with increasing heating time. Furthermore, the dispersant of $CaCO_3$ was better using the additive of $(NH_4)_2SO_4$ than that of NaH_2PO_4. These results demonstrated that the additives of NaH_2PO_4 and $(NH_4)_2SO_4$ not only had an effect on the phases, but also on the microstructure and shape in composites.

3.3. The thermal stability of the wood powder/$CaCO_3$ composites

The thermal stability of the wood powder/$CaCO_3$ composites was also investigated by TGA and DTA. TGA and DTA curves for the prepared samples at 160 °C for 24 h using the addition of NaH_2PO_4, Na_2CO_3, and $(NH_4)_2SO_4$ are shown in Fig. 8, respectively. From TGA curves, it is observed that the weight loss takes places at two stages: the first one (from 220 °C to 360 °C) is probably caused by thermal degradation of wood powder, and the other (from 360 °C to 600 °C) is probably caused by the decomposition of wood powder and $CaCO_3$ in composites (Zheng, Zhou, Du, & Zhang, 2002). The obvious weight losses of the wood powder/$CaCO_3$ composites prepared using the addition of NaH_2PO_4, Na_2CO_3, and $(NH_4)_2SO_4$ were ~55.1%, 59.1%, and 55.9% from 220 °C to 600 °C in the TGA curves, respectively. One can clearly see the corresponding exothermic peaks at about 347 °C, 350 °C, and 352 °C in the DTA curves, testifying that the TGA profiles are in good agreement with the DTA results of these samples.

4. Conclusions

In summary, we report the synthesis of the wood powder/$CaCO_3$ composites by hydrothermal method using the dewaxed wood powder. XRD and FTIR results indicated the successfully fabrication of the wood powder/calcite composites. SEM images showed that $CaCO_3$ with the particles, six-side-like shape, and cube-like shape were obtained, the size of $CaCO_3$ increased with increasing heating time, and the number of $CaCO_3$ decreased with increasing heating time. The wood powder/$CaCO_3$ composites were still obtained using the addition of NaH_2PO_4 or $(NH_4)_2SO_4$ instead of Na_2CO_3. Using addition of NaH_2PO_4, experimental results demonstrated that the wood powder/$CaCO_3$ composites as majority phases and hydroxyapatite as a minor phase were observed, the number of $CaCO_3$ cubes and congregates increased with increasing heating time. Therefore, additives of NaH_2PO_4 and $(NH_4)_2SO_4$ not only had an effect on the phases in composites, but also on the microstructure and shape. The thermal stability of all the samples had slight difference. Compared with cellulose-based composites, the wood powder composites can utilize all the main components of lignocelluloses.

Acknowledgments

Financial support from the National Natural Science Foundation of China (31070511, 31170557), Research Fund for the Doctoral Program of Higher Education of China (20100014120010), China Postdoctoral Science Special Foundation (201003059), Program for New Century Excellent Talents in University, and Major State Basic Research Development Program of China (973 Program) (No. 2010CB732204) are gratefully acknowledged.

References

Ashori, A. (2008). Wood–plastic composites as promising green-composites for automotive industries. *Bioresource Technology*, *99*, 4661–4667.
Bakraji, E. H., & Salman, N. (2003). Properties of wood–plastic composites: Effect of inorganic additives. *Radiation Physics and Chemistry*, *66*, 49–53.
Blanchard, V., & Blanchet, P. (2011). Color stability for wood products during use: Effects of inorganic nanoparticles. *Bioresources*, *6*, 1219–1229.
Cundy, C. S., & Cox, P. A. (2003). The hydrothermal synthesis of zeolites: History and development from the earliest days to the present time. *Chemical Reviews*, *103*, 663–701.
Dalas, E., Klepetsanis, P. G., & Koutsoukos, P. G. (2000). Calcium carbonate deposition on cellulose. *Journal of Colloid Interface Science*, *224*, 56–62.
Donners, J. J. J. M., Heywood, B. R., Meijier, E. W., Nolte, R. J. M., Roman, C., Schenning, A. P. H. J., et al. (2000). Amorphus calcium carbonate stabilized by poly(propylene imine) dendrimers. *Chemical Communications*, 1937–1938.
Fimbel, P., & Siffert, B. (1986). Interaction of calcium carbonate (calcite) with cellulose fibres in aqueous medium. *Colloids and Surfaces*, *20*, 1–16.
Fujita, S., Miyafuji, H., & Saka, S. (2003). Antimicrobial SiO_2 wood-inorganic composites as prepared by the sol–gel process with water-soluble silicon oligomer agents. *Mokuzai Gakkaishi*, *49*, 365–370.
He, Q., Huang, Z., Liu, Y., Chen, W., & Xu, T. (2007). Template-directed one-step synthesis of flowerlike porous carbonated hydroxyapatite spheres. *Materials Letters*, *61*, 141–143.
Jia, N., Li, S. M., Ma, M. G., Sun, R. C., & Zhu, J. F. (2010). Hydrothermal synthesis and characterization of cellulose-carbonated hydroxyapatite nanocomposites in NaOH–urea aqueous solution. *Science of Advanced Materials*, *2*, 210–214.
Jia, N., Li, S. M., Ma, M. G., Sun, R. C., & Zhu, J. F. (2012). Hydrothermal fabrication, characterization, and biological activity of cellulose/$CaCO_3$ bionanocomposites. *Carbohydrate Polymers*, *88*, 179–184.

Jiang, H. H., & Kamdem, D. P. (2004). Development of poly(vinyl chloride)/wood composites: A literature review. *Journal of Vinyl & Additive Technology*, *10*, 59–69.
Jokanović, V., Izvonar, D., Dramićanin, M., Jokanović, B., Zÿivojinović, V., Marković, D., et al. (2006). Hydrothermal synthesis and nanostructure of carbonated calcium hydroxyapatite. *Journal of Materials Science: Materials in Medicine*, *17*, 539–546.
Kuriakosea, T. A., Kalkuraa, S. N., Palanichamyc, M., Arivuolid, D., Dierkse, K., Bocellif, G., et al. (2004). Synthesis of stoichiometric nano crystalline hydroxyapatite by ethanol-based sol–gel technique at low temperature. *Journal of Crystal Growth*, *263*, 517–523.
Lai, S. M., Yeh, F. C., Wang, Y., Chan, H. C., & Shen, H. F. (2003). Comparative study of maleated polyolefins as compatibilizers for polyethylene/wood flour composites. *Journal of Applied Polymer Science*, *87*, 487–496.
Mai, C., & Militz, H. (2004). Modification of wood with silicon compounds, inorganic silicon compounds and sol–gel systems: A review. *Wood Science and Technology*, *37*, 339–348.
Miyafuji, H., Kokaji, H., & Saka, S. (2004). Photostable wood-inorganic composites prepared by the sol–gel process with UV absorbent. *Journal of Wood Science*, *50*, 130–135.
Nelson, D. G. A., & Featherstone, J. D. B. (1982). Preparation, analysis, and characterization of carbonated apatites. *Calcified Tissue International*, *34*, 69–81.
Okamoto, T. (2003). Recent developments in wood/plastic composites—Extrusion of wood-based materials. *Mokuzai Gakkaishi*, *49*, 401–407.
Selke, S. E., & Wichman, I. (2004). Wood fiber/polyolefin composites. *Composites Part A: Applied Science and Manufacturing*, *35*, 321–326.
Shen, J., Song, Z. Q., Qian, X. R., & Yang, F. (2010). Carboxymethyl cellulose/alum modified precipitated calcium carbonate fillers: Preparation and their use in papermaking. *Carbohydrate Polymers*, *81*, 545–553.
Stark, N. M., & Rowlands, R. E. (2003). Effects of wood fiber characteristics on mechanical properties of wood/polypropylene composites. *Wood and Fiber Science*, *35*, 167–174.
Subramanian, R., Maloney, T., & Paulapuro, H. (2005). Calcium carbonate composite fillers. *Tappi Journal*, *4*, 23–27.
Sugimoto, T. (1987). Preparation of monodispersed colloidal particles. *Advances in Colloid and Interface Science*, *28*, 65–108.
Vilela, C., Freire, C. S. R., Marques, P. A. A. P., Trindade, T., Neto, C. P., & Fardim, P. (2010). Synthesis and characterization of new $CaCO_3$/cellulose nanocomposites prepared by controlled hydrolysis of dimethylcarbonate. *Carbohydrate Polymers*, *79*, 1150–1156.
Zheng, H., Zhou, J., Du, Y., & Zhang, L. (2002). Cellulose/chitin films blended in NaOH/urea aqueous solution. *Journal of Applied Polymer Science*, *86*, 1679–1683.